201979: gold grain, Silica Hills prospect (Tozer Formation, Sholl Terrane)

Sample type	Gold grain
Total weight	0.3 g
Sample location	Silica Hills, about 25 km south of Karratha
Coordinates	Zone 50, MGA 492970E 7684191N
Datum	GDA94
1:250 000 map sheet	DAMPIER (SF 50-2)
1:100 000 map sheet	DAMPIER (2256)
Tenement	P 47/2093-S; E 47/1746-I
Collector	Artemis Resources Limited

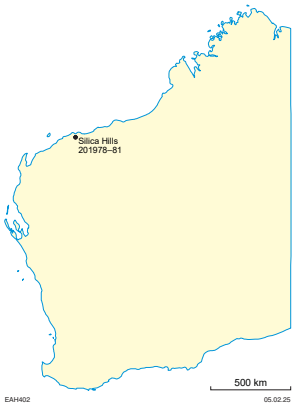

Location and sampling

The sample was provided by Artemis Resources Limited in January 2019. It was collected from the weathering profile above felsic rocks with quartz veining at the Silica Hills prospect, in the northwest Pilbara region (Artemis Resources Limited, 2019, written comm., 11 January).

Geological context

The Silica Hills prospect is located about 4 km south of the Sholl Shear Zone, a significant terrane-boundary in the Sholl greenstone belt of the Sholl Terrane of the northwest Pilbara Craton (Hickman, 2016; GSWA, 2020). The local bedrock includes metamorphosed rhyolite and dacite of the 3128–3116 Ma Tozer Formation (Hickman, 2021). Metamorphosed dolerite of the Tozer Formation outcrop about 0.1 km southeast of the sample locality, while Proterozoic dolerite dykes transect the area (GSWA, 2020).

Gold mineralization in the area is typically residual to eluvial and alluvial (e.g. Sholl Northeast 2 Eluvial, Mt Sholl Dryblowing 1, Mt Sholl B1 East (Cu), Specimen, and Silica Hills). Eluvial gold and gold-in-soil anomalies appear to have been derived from small, shallowly dipping quartz veins along lithological contacts (Bob Clynch and Associates, 1988). High-grade gold mineralization discovered in 2017 by Artemis Resources Limited at Silica Hills consists of coarse nuggety gold with high silver content in a quartz vein stockwork within a silicified intrusion along a shear zone (Artemis Resources Limited, 2017).

The nearest regolith landform is an alluvial–fluvial unit comprising unconsolidated clay, silt, sand, and gravel in active but poorly defined drainage channels on floodplains (GSWA, 2020).

Methodology

The gold sample was photographed and weighed, and its overall morphology and external features, such as colour, roundness, surface relief, coatings, mineral inclusions and mineral assemblages were recorded using visual morphometry. The raw surface of the sample was analysed using scanning electron microscopy with energy dispersive X-ray system (SEM-EDS). The sample was then mounted in epoxy resin, cut and polished, and the gold grain microstructure and inclusions were examined using reflected-light microscopy and SEM-EDS. Gold microchemistry was determined by laser ablation inductively coupled plasma mass spectrometry (LA-ICP-MS), calibrated against certified gold reference materials (CRM; Murray, 2009). The sample was ablated in quadruplicate along 0.5 mm-long traverses and average values calculated for elements present in the CRM. The gold surface was repolished after laser ablation, cleaned using ion beam milling, and its internal structure analysed using scanning electron microscopy with electron back-scattered diffraction (SEM-EBSD). Details of this method are described in Hancock and Beardsmore (2020).

Morphology

The gold grain is well rounded and slightly flattened, with dimensions 6 × 4 × 1.5 mm. It is extensively coated with non-compacted ferruginous clays which gives it a light brown colour (Fig. 1).

SEM-EDS analysis of raw surfaces

The surface of gold grain is spongy to flaky and intensely scratched and pitted but shows no compaction (Fig. 2).

Figure 1. Sample 201979: gold grain, Silica Hills prospect

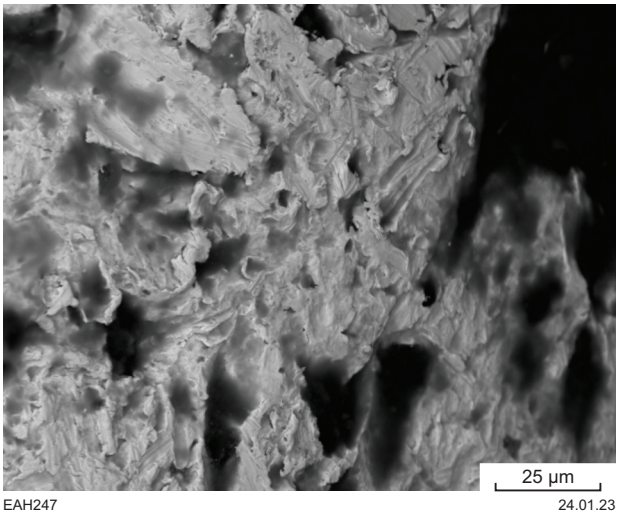

Figure 2. Backscattered electron image of part of surface of sample 201979: gold grain, Silica Hills prospect

Optical microscopy of polished surfaces

The polished section shows the smoothed but irregular shape of the gold grain, and the many deep, tortuous voids now filled with weathering-related ferruginous clays and small rounded quartz grains, but contain no fine, disseminated gold (Fig. 3). The voids were probably formed by preferential dissolution along intergranular, Ag-depleted gold veinlets.

SEM-EDS analysis of polished surfaces

The gold consistently contains 15% Ag. There are no depletion rims, nor Ag-free veinlets. The large voids are filled with granulated quartz and other regolith material (Fig. 4).

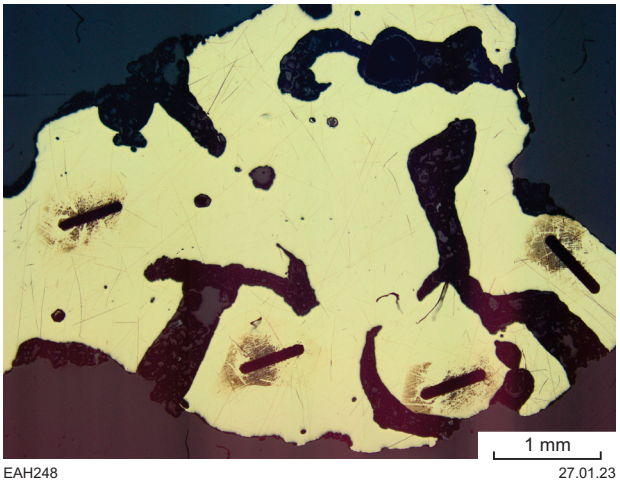

Figure 3. Reflected-light photomicrograph of cut and polished sample 201979: gold grain, Silica Hills prospect. Dark, elongate lines are laser ablation tracks produced during LA-ICP-MS analyses

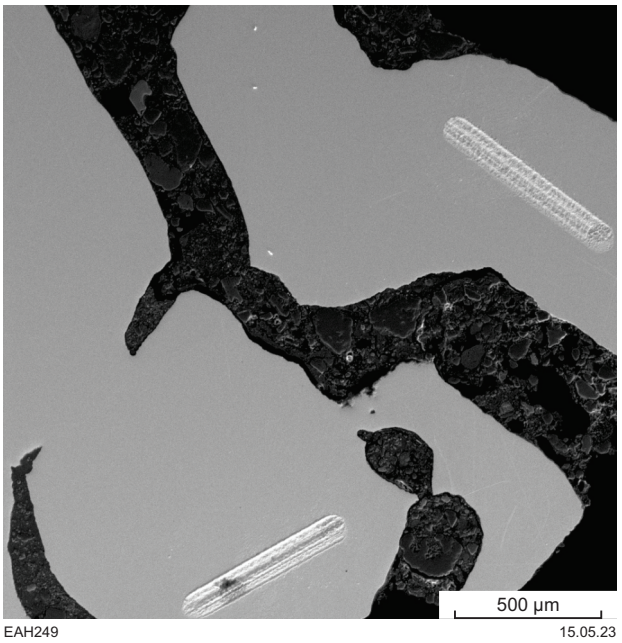

Figure 4. Backscattered electron image of part of polished surface of sample 201979: gold grain, Silica Hills prospect. Two bright, elongate lines are laser ablation tracks produced during LA-ICP-MS analyses

LA-ICP-MS analysis

Ag, Cu and Hg are consistently detected within the gold grain, in concentrations higher than the instrument detection limit, and probably occur as limited solid solutions in the gold. Ag content is high (10–13%), though somewhat lower than the 15% Ag detected using SEM-EDS. Cu and Hg are lower (87–126 ppm and 76–97 ppm, respectively; Table 1).

Mg, Ni, Zn, Sn, and Sb are also consistently present in the gold grain, but below detection limit (in sub-ppm) (Table 2), and, possibly occur in micro- and nano-inclusions. Unusually high abundances of lithophile elements, such as Na, Al and Nb detected in ablation traverses 1, 3 and 4, suggest the presence of rock-forming micro-inclusions.

Table 1. LA-ICP-MS data for main elements (above detection limit) in four traverses for sample GSWA 201979: gold grain, Silica Hills prospect

Ag (%)	*Cu (ppm)*	*Hg (ppm)*	*Other elements (ppm[1])[2]*
12	126	76	
13	87	97	
11	120	92	
10	125	90	

NOTES: 1 see Table 2 for concentrations and detection limit
2 results are only shown where standards are available for the element

SEM-EBSD analysis

Etching with HCl acid failed to produce a useable surface due to a strong reaction with Ag in the gold to form an obscuring AgCl 'passivation'. The cut surface was therefore etched using ion beam milling and analysed using SEM-EBSD. This revealed a completely recrystallized, coarsely granular microstructure (Fig. 5). Subgrain edges and twin planes are curved, bent and otherwise damaged, and internal crystal lattices are commonly deformed. The grain is extensively disaggregated along sub-grain boundaries. There are no secondary alteration rims or veinlets.

Interpretation

The gold contains no micro-inclusions such as were detected in other specimens from the Silica Hills prospect, but its coarsely granular, high-Ag character indicates that it is of primary hydrothermal origin, probably forming from a chloride-rich brines. Subsequent deformations, hydrothermal and burial alteration processes caused Ag dissolution along intergranular veinlets, gold grain recrystallization and partly disintegration creating deep voids filled with regolith material. There is no evidence of the surficial alteration during weathering.

Acknowledgements

The authors gratefully acknowledge Michael Verrall (CSIRO) for his help with the SEM/EDS/EBSD operation and data interpretation, and samples preparation for EBSD analysis. We thank Professor John Watling for discussions to improve the LA-ICP-MS data interpretation.

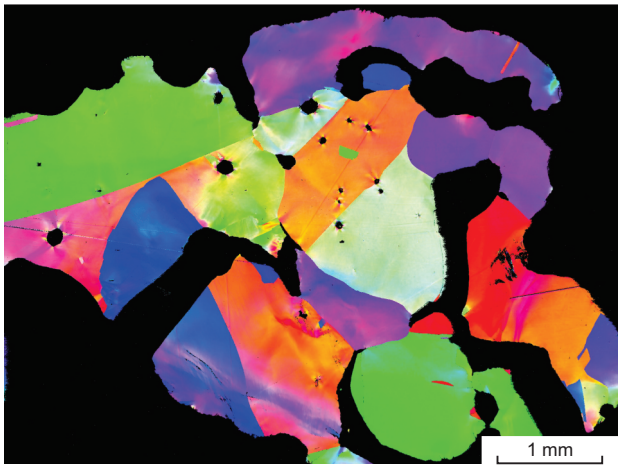

Figure 5. Reflected-light photomicrograph, after repolishing and acid etching, of sample 201979: gold grain, Silica Hills prospect

Table 2. LA-ICP-MS compositional data for sample GSWA 201979: gold grain, Silica Hills prospect

Laser ablation track	*Unit*	*^{7}Li*	*^{9}Be*	*^{11}B*	*^{23}Na*	*^{25}Mg*	*^{27}Al*	*^{29}Si*	*^{44}Ca*	*^{45}Sc*	*^{49}Ti*	*^{51}V*	*^{53}Cr*	*^{55}Mn*	*^{57}Fe*	*^{59}Co*	*^{60}Ni*	*^{65}Cu*
1	cps		2		5332	55	553						2			4	24	15601
2	cps					35	262			4	12	10	3		5	10	5	10792
3	cps		1	14	1080	133	936		46		8	11	3		5	5	18	14814
4	cps		1		1170	106	1398		83	1	11	5	7	119		47	12	15452
1	ppm					0.66											0.24	126
2	ppm					0.41					0.25						0.05	87
3	ppm					1.59					0.17						0.18	120
4	ppm					1.26					0.23						0.12	125
*DL**	*ppm*					*3.3*					*1.5*		*1.7*		*3.4*		*2.9*	*1.5*

Laser ablation track	*Unit*	*^{66}Zn*	*^{69}Ga*	*^{72}Ge*	*^{75}As*	*^{82}Se*	*^{85}Rb*	*^{88}Sr*	*^{89}Y*	*^{90}Zr*	*^{93}Nb*	*^{98}Mo*	*^{101}Ru*	*^{103}Rh*	*^{108}Pd*	*^{109}Ag*	*^{111}Cd*	*^{115}In*
1	cps	36	4	5			7	7		1	56	1		1	3	24654671	2	
2	cps	10	1		2		4				6	1			4	26846976	2	3
3	cps	52	5	3	3		4			1	35	2		3	3	23584475	3	
4	cps	25	5	2	5		1	4	2		14	1	1	2	5	20232133	4	
1	ppm	0.41													0.02	119625		
2	ppm	0.11			0.02										0.03	130262		
3	ppm	0.59			0.03										0.02	114432		
4	ppm	0.29			0.06										0.03	98167		
*DL**	*ppm*	*5.3*			*2*	*3.1*								*1.5*	*1.8*	*2.4*		

Laser ablation track	*Unit*	*^{120}Sn*	*^{121}Sb*	*^{126}Te*	*^{133}Cs*	*^{138}Ba*	*^{139}La*	*^{140}Ce*	*^{141}Pr*	*^{145}Nd*	*^{151}Eu*	*^{157}Gd*	*^{159}Tb*	*^{162}Dy*	*^{165}Ho*	*^{167}Er*	*^{169}Tm*	*^{172}Yb*
1	cps	160	67	3	6	5		2		2								
2	cps	95	71	2	3	1	2	1		3	1	2		2		2		2
3	cps	67	72	2	2	4		2		2		2	2		1			
4	cps	72	65	3	4	3							3				1	
1	ppm	0.72	0.26	0.05														
2	ppm	0.43	0.28	0.03														
3	ppm	0.30	0.28	0.04														
4	ppm	0.32	0.25	0.06														
*DL**	*ppm*	*1.6*	*2.8*	*5.6*														

Laser ablation track	*Unit*	*^{175}Lu*	*^{178}Hf*	*^{181}Ta*	*^{182}W*	*^{185}Re*	*^{189}Os*	*^{193}Ir*	*^{195}Pt*	*^{202}Hg*	*^{205}Tl*	*^{208}Pb*	*^{209}Bi*	*^{232}Th*	*^{238}U*
1	cps			3				1	1	21905	1	20	3		3
2	cps				2					28219		11	8		
3	cps							1		26802		7	2		4
4	cps			1				1		26102	1	52	6	2	2
1	ppm								0.01	76		0.06	0.01		
2	ppm									97		0.03	0.02		
3	ppm									92		0.02			
4	ppm									90		0.16	0.01		
*DL**	*ppm*								*2.5*	*2.5*		*1.5*	*2.2*		

NOTES: cps, count per second; ppm, parts per million; DL, detection limit
*****Detection limits have been determined using AuRM Reference Gold Standards (London Bullion Market Association). Standards were analysed nine times each and an average 2σ (95% Confidence Interval) Limit of Detection determined. Some results given in the text are quoted as values that are below the detection limit for these analytes. These values must be considered as "for information" only.

References

Artemis Resources Limited 2017, High Grade Gold Mineralisation identified at Silica Hills; Karratha, Western Australia (media release): Australian Securities Exchange (ASX), released 28 August 2017, 6p.

Bob Clynch and Associates 1988, Brady's Prospect, Final Surrender Report for the period 21/02/1986 to 29/06/1990, P47/400 prepared for Mr R Brady: Geological Survey of Western Australia, Statutory mineral exploration report A27188, <www.demirs.wa.gov.au/wamex>, 58p.

Geological Survey of Western Australia 2020, Northwest Pilbara, 2020: Geological Survey of Western Australia, Geological Information Series, data package (USB).

Hancock, EA and Beardsmore, TJ 2020, Provenance fingerprinting of gold from the Kurnalpi Goldfield. Geological Survey of Western Australia Report 212, 21p.

Hickman, AH 2016, Northwest Pilbara Craton: A record of 450 million years in the growth of Archean continental crust: Geological Survey of Western Australia, Report 160, 104p.

Hickman, AH 2021, Tozer Formation Formation (A-WHt-xb-f): Geological Survey of Western Australia, WA Geology Online, Explanatory Notes extract, viewed 04 January 2023, <www.demirs.wa.gov.au/ens>.

Murray, S 2009, LBMA certified reference materials. Gold project final update: The London Bullion Market Association, Alchemist, no. 55, p. 11–12.

Recommended reference for this publication

Hancock, EA, Blay, OA and Beardsmore, TJ 2025, 201979: gold grain, Silica Hills prospect; GSWA Mineralogy Record 13: Geological Survey of Western Australia, 5p.